H^- EXTRACTION AND PROTON ACCUMULATION FOR THE TRIUMF KAON FACTORY SYNCHROTRON PROJECT

G.H. Mackenzie
TRIUMF, 4004 Wesbrook Mall, Vancouver, B.C., Canada V6T 2A3

Summary

The proposed TRIUMF KAON factory accelerator complex includes the accumulation of the cw cyclotron beam in an appropriately designed storage ring. Ions accumulated over 20 ms would be transferred to a rapid cycling, 50 Hz, booster synchrotron in one turn. The most appropriate method to fill the accumulator ring is by charge exchange injection, $H^- \rightarrow H^+$, together with so programming the incoming beam energy and direction and the ring closed orbit location that precessional motion fills the acceptance with a broad smooth distribution. The results of computer simulations are presented. An experimental program has successfully demonstrated the feasibility of efficient extraction of 450 MeV H^- ions from TRIUMF. Spill on the septum of an electrostatic deflector is eliminated by a thin stripping foil placed upstream. The extraction efficiency is increased by generating a coherent radial oscillation at $\nu_r=3/2$ by means of a radial rf field. A 10 mm space between deflected and circulating beam was measured at the location of a planned magnetic channel; the deflector/foil transmission was 85%.

Introduction

TRIUMF has proposed[1] that a post-accelerator be constructed with the existing 520 MeV H^- cyclotron serving as injector. The system would incorporate a moderately rapid cycling 10 Hz synchrotron with a 50 Hz booster synchrotron to deliver 100 μA to 30 GeV.

The time available for injection into a rapid cycling synchrotron is only a few % of the repetition time, say ≤0.5 ms at 50 Hz. An average current of 100 μA corresponds to 1.25×10^{13} protons per booster cycle; the current during the injection interval would be ≥4 mA. A typical cw cyclotron beam of ~ 0.1 mA needs to be accumulated during most of the booster period and then injected. Several techniques have been discussed[2] for accumulation within a cyclotron. They involve some means to reduce the rate of acceleration followed by a periodic deflecting kick at the accumulation radius. Tolerances on machine stability restrict accumulation to hundreds of turns only (2-20 μs) and require rapid kicker operation ~100 kHz. The ASTOR concept[3] exemplifies a device specifically designed to accelerate and stack, by means of phase expansion, intense proton beams from a cyclotron. The maximum accumulation time appears to be limited to ~ 1 ms.

Accumulation and beam transfer processes must be efficient. Hands on maintenance requires an average loss ≤ 1 nA/m; a local loss of 3 μA would be similar to that from a "thin" 10 mm meson production target and require remote handling and 3-4 m shielding.

The booster acceptance is 2×10^4 times larger than the TRIUMF emittance, Table 1, in order to restrict the maximum space charge tune shift to ≤ 0.2. This cannot be fully expoited by proton injection since the efficiency of deflection into transverse phase space or RF stacking falls considerably after ~10 turns. Charge exchange injection allows continual injection into the same macroscopic piece of phase space with the incoming particles entering interstitial spaces among the previously injected particles. This offers the best opportunity for an efficient injection process over thousands of turns and requires the extraction of H^- ions intact from TRIUMF. This possibility was envisaged during the design[4] and two exit horns (vacuum tank protrusions between pole return yokes) were widened to accommodate H^- beam.

Table 1. Machine Parameters

	TRIUMF Cyclotron†	Accumulation Ring	Booster Synchrotron
Energy (GeV)	0.45	0.45	0.45-3.0
Frequency (ion) MHz	4.6	1.02	1.02-1.36
Frequency (rf)/Harmonic	23/5	46.1/45	4.61-61.1/45
$(\Delta E/turn)/V$ (MV)	0.29/0.3	0/0.57	0.21/0.60
(Future)	0.9/0.9		
ΔR/turn (mm)	1.4	-	-
Emittance/Acceptance			
Horizontal (μm)	1.5	75	75
Vertical (μm)	2	25	37.5
Longitudinal (eVs)$\times10^{-3}$	3.1	48	48
Betatron frequency			
Horizontal	1.52	5.2	5.22
Vertical	0.22	7.2	7.2
Synchrotron frequency	-	0.045	0.043-0.005
Orbit Radius (m)	7.2	34.1	34.1
Beam pipe aperture			
Horizontal (mm)	Large	66	79
Vertical (mm)	±30	31	44

†Parameters for high current operation at the accumulation energy of 450 MeV.

Cyclotron Extraction

Extraction procedures were reviewed by Joho[5] in 1969. When turns are not completely separated a large radius gain per turn reduces loss on the septum of the first element, usually an electrostatic deflector. This may be achieved by a large energy gain per turn, extraction at an integer resonance with a moderately large magnetic integer harmonic, or extraction beyond an integer resonance exploiting precession of a coherent amplitude produced at the resonance or at injection. At TRIUMF separated turns are seen at ~250 MeV but are not expected at 450 MeV in the near future. Extraction much below 450 MeV introduces technical problems in booster synchrotron rf swing requirements and in the amount of deflecting power needed in the cyclotron.

Fortunately acceleration of H^- or partially stripped ions permits the generation of separated turns at the point of extraction. A stripping foil with a width, w, less than the radius gain per turn, will convert H^- to H^+ (or A^{n+} to $A^{(n+m)+}$). Protons will curve out of the primary beam to produce a gap, Fig. 1. A gap will recur every π/ν_r, gradually filling in as the phase band generates an energy difference, and the phase space precesses. Thus the septum should follow the foil within one or two turns. The length, 2ℓ, of the beam free region in the azimuthal direction is $w/\gamma^2 A_i$ where the divergence, x', may be written as $\gamma^2 A_i$ for a matched beam with incoherent amplitude A_i. Figure 1 shows the situation for the conservative case of the septum following immediately upon the foil. Space must also be left for clearing the stripped beam, with radius of curvature ρ_s, and at this location the beam free length is reduced by $(2w\rho_s)^{1/2}$. The beam free length at following gaps may be longer and contain no H^+, but their size is more dependent on variations in cyclotron tune.

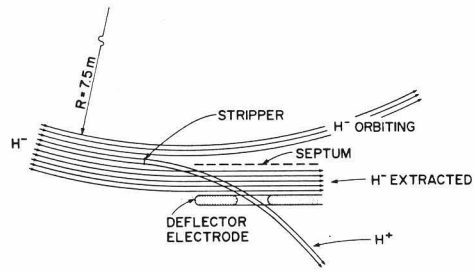

Fig. 1. Illustration of action of a foil shadowing a deflector septum. The working protype allows the H^+ beam to pass in front of the deflector electrode and through a hole in the support and service frame.

It is desirable to position the foil so that the stripped beam leaves the cyclotron at a port. This reduces machine activation and also provides a beam of superior quality for experimental use. The extraction efficiency, assuming no loss on the electrostatic deflector or subsequent elements, will be $(\Delta r - w)/\Delta r$; where Δr is the turn separation. Since the minimum value of w is set by the beam divergence and deflector size and strength the efficiency still depends on generating a large Δr (larger than for a septum alone whose projected thickness would be much less than the foil width). The efficiency now, however, refers solely to the preservation of H^- ions. The sum of both beams can still be 100% and activation and ionisation much reduced.

Improvement of Extraction Efficiency

Two methods have been investigated, the first proposed to place additional accelerating cavities around the machine circumference, the second to create a coherent radial oscillation and exploit precessional extraction beyond $\nu_r \approx 3/2$. The former increases the radius gain per turn overall, the latter locally. It is anticipated that the initial effective width of the septum may be 0.3 mm. For x' of 0.5 mr a 1 mm foil shadows the septum and provides clearance for the stripped H^+ beam. The maximum H^+ current that can be accommodated in a beam line, targets and dump without going to remote handling and use of radiation hard components is 10 μA. An efficiency of more than 90% is then required to deliver 100 μA H^- to the KAON Factory. Of course the system illustrated in Fig. 1 can provide more than 10% H^+. A wide foil, possibly rotating about a vertical axis, could deliver ~100 μA to a present meson production line while allowing a few μA of H^- to be extracted for commissioning purposes.

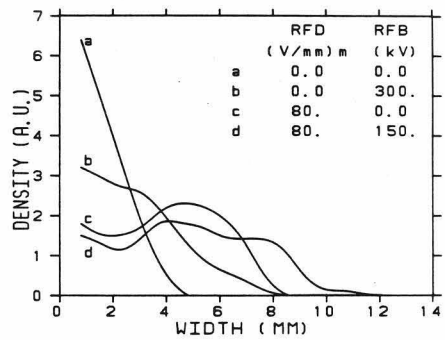

Fig. 2. Radial width of extractable beam. For combinations of resonance driver (RDF) and auxiliary cavity (RFB). The latter increases ΔT/turn from 0.3 MeV to 0.6 MeV d) and 0.9 MeV b)

Figure 2 illustrates the beam density across the surface of a supposed target located at the entrance to an electrostatic deflector. (A_i assumed 1.4 mm). The fraction extracted as H^+ is given by the mean density from width 0 to w. An increased H^- extraction efficiency is associated with a greater H^- beam width. The latter is largely due to dispersion and a septum shadowing foil extracts an energy width less than ΔT, the energy gain per turn.

Auxiliary Cavities. The choice of cavity shape is discussed in Ref. 6. An azimuthal length of $\beta\lambda/2$ accelerates ions entering and leaving. The radial length is approximately $\lambda/4$. The main accelerating frequency (23 MHz) is itself the 5th harmonic, h=5, of the ion orbit frequency and a superharmonic of this was chosen to keep the cavities small and the power low. The 92 MHz design shown in Fig. 3 has the peak voltage at the outer radius to provide an abiabatic acceleration. Compression arises from $B_z(t)$ at the shorting plane. The upper section is attached to the lid, the lower to the tank floor. The size, and consequently the harmonic, must provide both adequate increase in acceleration at 450 MeV and continued acceleration to beyond 500 MeV when the extraction system is unused. Parameters of possible cavities are summaried in Table 2. Under existing conditions, more than 100 μA is contained within ±16° of rf phase (23 MHz). A threefold increase in energy gain would compress this to ±5.3°, reduce the phase wander, and also reduce the electromagnetic stripping loss to 500 MeV from ~15 to 5%. A choice may be made between reduced tank activation, increasing the beam intensity at 500 MeV with present activation or increasing the maximum operating energy to increase high energy pion flux.

An h=15 cavity was rejected because of size and remote handling, and power dissipation. The h=25

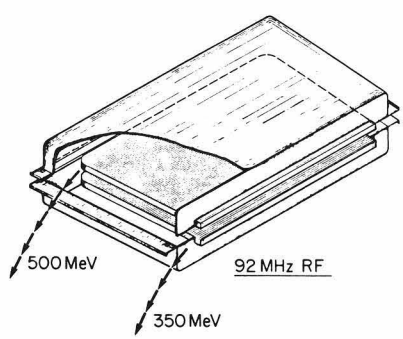

Fig. 3. Auxiliary accelerating cavity.[9]

Table 2. Auxiliary Cavity Parameters

h'(main rf) /MHz	Peak Volts (kV)	kV at 450 MeV	$\beta\lambda/2$ (m) r_{max}, r_{min}	Power kw
5(115)	100	100	1.0, 0.93	90
4(92)	120	100	1.26, 1.12	160
3(69)	180	160	1.67, 1.44	250

harmonic cavity is less efficient at 450 MeV and two cavities are required to produce enough phase compression for stable operation.

Precessional extraction. It would appear that, without a quintupling of the energy gain per turn, the radial betatron frequency, ν_r, cannot approach integer values without significant phase slip, or vertical defocusing in the case of ν_r=2. Hence TRIUMF must exploit ν_r=3/2, at 428 MeV, the closest resonance to the preferred energy. To date only electrostatic or static magnetic systems have been used as the major driving force for particle extraction, although rf fields have been used to drive betatron oscillations in the "knock-out" technique of tune measurement.

The angular extent of one radial oscillation is $2\pi/\nu_r$, when ν_r=1.5 the co-ords (x,x') have mirror values (-x,-x') on alternate turns. Figure 4 illustrates how a coherent radial amplitude can be generated and made to grow by applying a radial kick alternating in sign each turn. For h = 1, $\omega_{kick}=\omega_{ion}/2$, and the situation is equivalent to the generation of a coherent amplitude at ν_r=1 except that an oscillatory driving field must be used. The effective width of the resonance will be $1/(d\nu_r/dn)^{1/2}$ which, for an isochronous machine may be written $\{E_0/(dT/dn)\}^{1/2}$ since $\nu_r \approx \gamma$. For TRIUMF dT/dn is 0.3 MeV/turn, giving a width of 56 turns. This corresponds to 78 mm and is so much larger than the incoherent betatron amplitude that

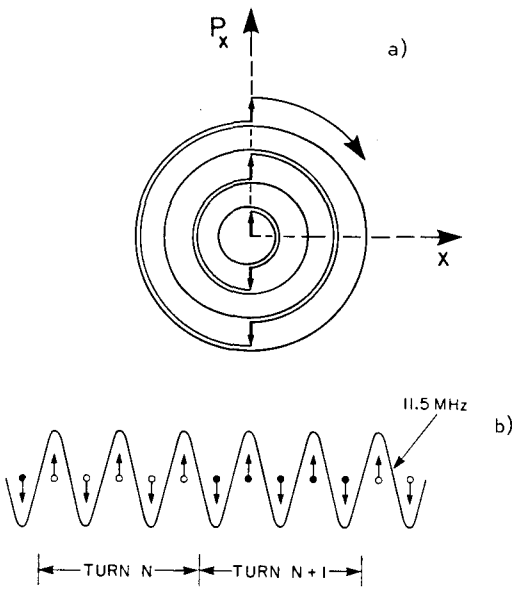

Fig. 4. Illustration of the effect of turn by turn kicks of opposite sense. a) for a single particle in phase space; b) for ions accelerated by a 5th harmonic of the rotation frequency.

all particles acquire the same additional amplitude and the motion is linear.

Where the accelerating RF field has h=1 and where separated turn conditions apply the radius gain/turn contribution from a given A_c and $\nu_r \approx 3/2$ is twice that for $\nu_r \approx 1$; since at a given azimuth, alternate turns are displaced inward. A square wave field would retain this feature when h > 1. This can be achieved but is, at the moment, irrelevant for TRIUMF since neither the phase band populated nor the machine stability satisfies separated turn criteria. An 11.5 MHz field ($f_{rf}/2$) will give each bunch an alternate deflection of the same magnitude. However alternate bunches and alternate turns of the same bunch are deflected in the opposite sense; this halves the effective turns separation. The principle is illustrated in Fig. 4a,b and the progression of a pair of particles in Fig. 5. The amplitude gained is proportional to the product of the average kick and number of turns in the resonance region, ~17 MeV wide. This varies with particle phase as $\{\cos(\phi/2)\}/\cos\phi$ and lies between 1.08 and 1.00 for a bunch ±25° wide. An increased coherent amplitude A_c increases both the turn spacing and the excursion C, Fig. 5; the latter may prevent utilisation of the former. Sector focussing causes the detail of Fig. 5 to alter with cyclotron azimuth; for large A_c the outward displacement of A, A' may encroach, at other angles, on the trajectory of B_E. Both determine A_c^{max} and hence the driving strength required.[7]

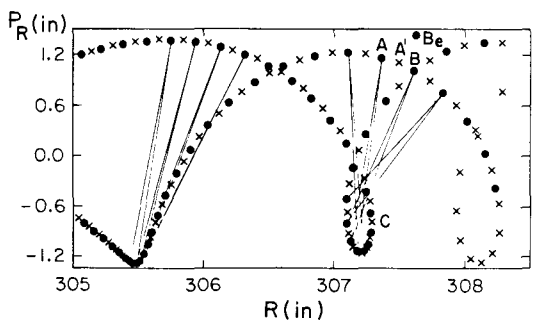

Fig. 5. Radial motion of the 2 particles classes shown at the driver azimuth. Heavy dots are particles receiving an initial outward kick on entering the device. The light lines connect adjacent turns and are to guide the eye. The crosses are particles receiving an initial inward kick. $E_r.\ell$=40 (V/mm)m. Turns are shown from 462 to 481 MeV. B is an extractable turn with an enhanced displacement from A and A', C is the maximum outward excursion on previous turns. B_E corresponds to B after an impulse deflection.

The principle can be applied at any value of ν_r (or ν_z). However the efficiency of transferring power to the beam is greater near a resonant value of ν, e.g. 1/2, 4/3, 5/4 etc; a single driver is most efficient when ν=0.5*m. Elsewhere a pair of coupled drivers with appropriated modulation may be considered. The deflection x' (mr) for a singly charged particle E_0 (GeV) and a field E_r (kV/mm) over orbit length ℓ is $\{\arctan(E\ell/E_0\beta^2\gamma\}$ milliradians; multiplication by $\beta\gamma R_{cu}$ gives a value in cyclotron units. TRIUMF benefits, in this case, from a large R_{cu}, of 10.2 m. A typical density distribution is illustrated in Fig. 2.

Generation of deflection

Ordinarily deflection occurs near the fringe field, this serves to direct the orbit further toward ν_r=0 where it naturally swings out. The farther the

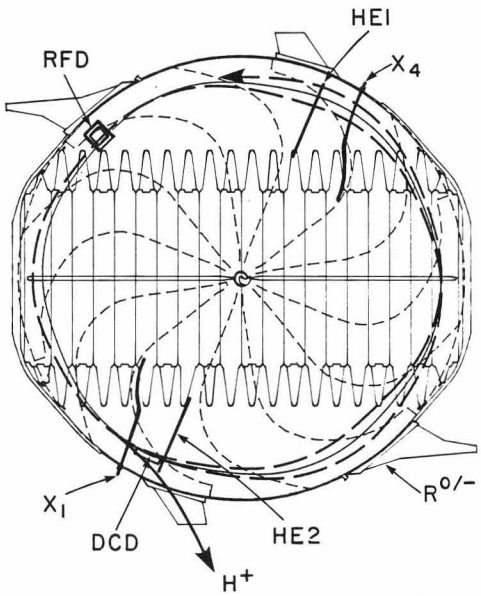

Fig. 6. Plan view of cyclotron vacuum tank showing the location of components for a recent experiment and a 450 MeV orbit with the radial amplitude exaggerated. RFD=Resonance Driver, DCD=electrostatic deflector, HE1 and 2 are vertical and differential radial probes, X_1 and X_4 are stripping foils. $R^{0/-}$ a recess to accommodate "tangential" beams.

starting point from ν_r=0 the harder it is to achieve this unwinding. In the case of TRIUMF we propose to deflect into a field that is still increasing with radius.

It can be seen from the plan view of the vacuum tank, Fig. 6, that the maximum free space between the rear of the resonator levelling arms and an exit port is 105°. The radial interval from 450 MeV to the main magnet coil where the field reverses sign, is 1 m. Extraction over a 90° segment is equivalent to a radius of curvature increase of 0.72 m or a decrease in field of 0.05 T over 12 m, B_z hereabouts is 0.48 T. An active channel, which may be turned off for movement or for machine tuning, is preferred. A field reduction of 0.1 T next to a current sheet requires a current of 1 kA and a wall thickness of 12 mm if hollow, water cooled conductors are used. Such a magnetic septum could not be used as the initial deflecting element and must be preceded by electrostatic deflectors. An electrostatic deflecting field of 60 (kV/mm)m is required should the magnetic channel above follow immediately upon the deflector. A series of weaker elements located near betatron oscillation maxima may be used. For example a deflector field of 2(kV/mm)m if the magnetic channel is located 60° downstream. Such a sequence reduces the space available for the channels and increases their field requirements to 1.5 Tm. It requires extraction over 1.5 turns since regions occupied by major equipment (such as resonators) and regions where the deflected orbit displacement is negative can not be used. An example layout may be seen in Ref. 7.

Prototype Extraction Equipment

Operating prototypes of components are being built with the intention of installing them in the cyclotron for short, typically 3 day, experiments with beam. These take place during semi-annual shutdowns. The program is intended to confirm calculations of beam behaviour and component characteristics to check performance in the cyclotron and to measure effects too difficult to predict, either because of insufficient data or extreme sensitivity. To date experiments have been performed with the resonance driver and electrostatic deflector. An auxilliary cavity and associated power amplifier are being constructed and a septum magnetic channel designed.

The operating environment includes maintaining a tank pressure better than 10^{-7} Torr. A flux of energetic neutral atoms of 4×10^8/mm^2 with energies ranging up to the extraction energy and rf leakage of 5 V/mm. Devices spanning the median plane must be both radiation resistant and remotely handleable. A technique to retract deflectors and channels beyond the 520 MeV orbit has been devised but not implemented for these prototypes. A general purpose vacuum chamber with the same inner height as the cyclotron, 0.4 m, has recently been constructed to check equipment operation before installation and for engineering physics research and development. A C-shaped magnet may be rolled forward to encompass one third of the chamber length in a field up to 0.45 T.

Resonance Driver

This consists of a hollow flat U-shaped electrode mounted at the end of the inner conductor of a capacitively foreshortened vertical transmission line, Fig. 7. The 11.5 MHz electric field, E_R, is developed between the tip of the U and the similarly shaped grounded structure enclosing it. The mid-point of the gap lies on the ν_r=3/2 resonance at 428 MeV, 7.51 m radius. Ample voltage is available so the radial extent of the field, 127 mm, exceeds the resonance width of 78 mm to allow for uncertainties in absolute position of ±3 mm and to improve the validity of those elementary calculations that assume E_r constant.

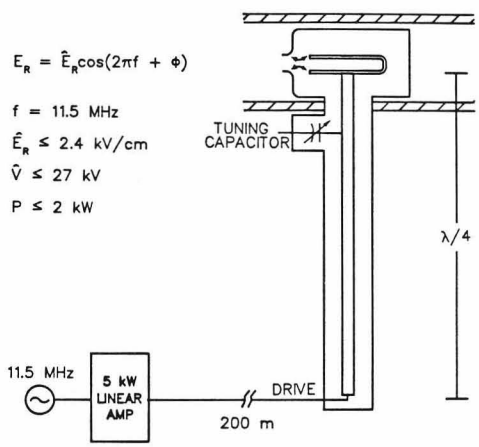

Fig. 7. A schematic illustration of the resonance driver, transmission line, and amplifier. The resonance is located where the field $E_r(t)$ develops between the centre and ground electrodes.

The vertical limb at the rear of the U lies beyond 520 MeV. This allows acceleration into the field free region to develop precession when the device is energized, and to permit normal cyclotron operation when off. The prototype[8] has been operated for over one year. The 5 kW supply generated a peak electrode voltage of 40 kV in the laboratory with no insulator breakdown. The maximum in the cyclotron is 25 kV, probably because of losses in the 200 m flexible transmission line. This value is just above that to produce A_c^{max} and consequently there has been no immediate need to increase power transmission efficiency.

Electrostatic Deflector[9]

The grounded septum is made of molybdenum strips 5 mm wide, 7 mm centre to centre, and pre-tensioned to 70 N. The strips are 0.07 mm thick and the positional scatter about the computed trajectory is $\leq \pm 0.1$ mm. The positive anti-septum is 0.85 m long, 50 mm tall and separated from the septum by 13 mm. This gap is greater than the beam width generated by the resonance driver but can accommodate the additional width generated by an accelerating cavity, Fig. 2. The anti-septum is formed from a thin 0.8 mm stainless steel skin moulded into three horizontal tubes for rigidity. The tubes, 0.8 mm wall thickness, carry nitrogen gas as coolant. The electrode is supported on two hollow $A\ell_2O_3$ insulators, the gas entering and leaving by this means. The prototype length, 0.85 m, is constrained by an existing beam probe at the test location. The connection to the positive voltage dc power supply is also through the insulator and gas feed line so that the lead is at atmospheric pressure throughout its length. The feedthrough ports are in valleys, which occupy about one-third of the cyclotron circumference, whereas the ideal deflector position may be in a hill. In addition the deflector is adjustable in radius and pivot angle about the first septum foil. This system of electrical connection is mechanically more flexible than the use of a separate vacuum feedthrough together with support of the positively biased conductor on insulating standoffs with radiation shields and electron traps. On the other hand the working positive voltage is presently limited to +40 kV. The characteristics of this system are being studied in the development chamber.

Magnetic Channels

Conceptual designs[10] have been made for a low field, 0.08 T, narrow septum model and a high field, 0.3 T co-axial model magnetic channels, Fig. 8. Such devices have been used elsewhere. The TRIUMF environment influences the choice of material and imposes tight constraints on the fringe fields; in particular a gradient of 0.02 Tm^{-1} observably affects vertical focussing. Calculations made using the two dimensional code GFUN showed that the presence of magnet iron does not much alter the predictions of the three dimensional calculations based on current distributions alone.

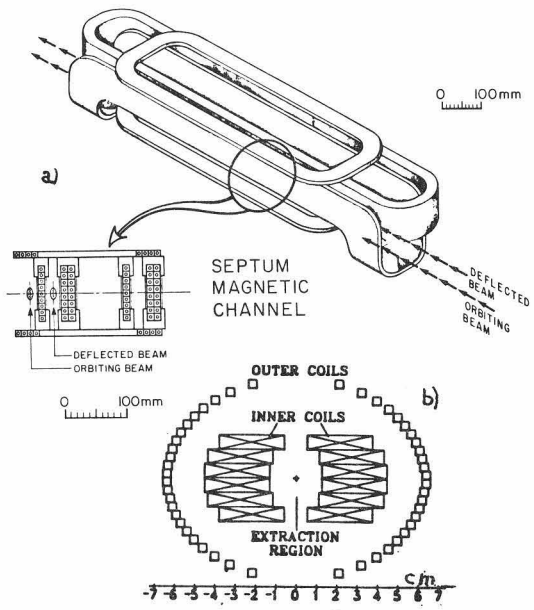

Fig. 8. Magnetic channels. a) a view and section of the septum channel, 480 A and 700 A producing central ΔB_z of 0.08 T. b) Section through a co-axial channel, 0.6 and 1.3 kA produce ΔB of 0.3 T.

The narrow septum, Fig. 8a, is necessary to capture the H^- beam from electrostatic deflectors. The septum coil makes a vertical excursion beneath the compensating coil at the entrance and exit to accommodate remote handling from above. This asymmetry produces transverse field components, up to ~0.05 T but their integral through the deflector is close to zero. These fields are included in our orbit codes along with the additional B_z (R,θ) and the final effect on the beam, provided it comes no closer than 1 mm to the edge of the septum coil, is a vertical displacement of 0.5 mm and almost no distortion of radial or vertical phase space. A separation of 0.13 m between extracted and circulating beam is expected 60° downstream. Such a drift may prevent installation of a strong channel and a more powerful septum channel(s) followed closely by a co-axial version may be necessary.

The design assumes 11 mm square, hollow, water-cooled copper conductors. The current required in the two main coils is 700 A and 480 A, and for short experimental tests will be obtained from a single, available, power supply with the addition of an active shunt between the coils. The present assembly scheme involves installing insulating strips, eventually radiation resistant alumina, between turns while winding. Stainless steel clamps, trepanned in the beam plane to 1 mm thick would be installed to give an overall septum thickness of 15 mm. See detail in Fig. 8.

The coaxial magnetic channel is based upon two hollow concentric current-carrying tube-like structures, 130 and 55 mm diameter. They would be constructed from hollow water-cooled copper windings, the winding density varying in a cos $n\theta$ manner. Currents of ± 0.63 and ∓ 1.31 kA flow in right and left halves of the tubes to produce a homogeneous 0.3 T field reduction along the common axis. The two halves of both tubes are connected by conductors taken vertically above and below the beam in a saddle coil arrangement. The balanced, enclosed, construction, Fig. 7b, minimizes the leakage field which is a fairly uniform 12 G in the region of the circulating beam. This is easily compensated by low power trim coils. The total power would be ~65 kW.

Auxiliary Accelerating Cavities

Development is proceeding in two stages. In the first a "warm," moderate power 25 kW full scale model has been built.[9] This originally was a "cold" model with a moveable short adjusted to determine experimentally the cavity length resonating at 92 MHz and to measure the Q, (=9000), and other properties at signal level. At present experiments are refining the design of the coupling loop and tuning system. Manufacturing drawings for the second stage, the 120 kW/120 kV cyclotron cavity, will then be completed.

In parallel with this program the power amplifier,[8] based on an EIMAC Y567B tetrode, is being constructed, and measurements are being made on the anode tuning cavity. The driver stage is a 10 kV commercial transmitter. Initially high power commissioning will utilize a water-cooled dummy load. Then the "warm" cavity and amplifier will be coupled with a relatively short transmission line and the system developed in the laboratory until a high power cavity is available.

Extraction Computations

Standard equilibrium orbit and general orbit codes are used. The magnetic field description does not assume symmetry about the geometric mid-plane but

incorporates the transverse field components, B_r and B_θ, and (dB_z/d_z) measured in 1974. Regions of space (r,θ) may have theoretical electric and magnetic fields described in finer detail and the equations integrated over shorter steps.

A Monte Carlo COMA tracks up to 2,000 particles using linear matrices obtained from the E.O. Code. Accelerating forces are condensed to local impulses. The code is particularly useful where no turn separation exists and probe measurements reveal a homogeneous particle density. Not only is the distribution in the cyclotron available but also the particle properties and correlations. The same are given for beam hitting a segmented probe head or foil. Observations of the accelerating beam may then be made by comparing measured and calculated probe currents or extracted beam properties.

Experiments

The first measurements were of the properties of the resonance driver, the formation of a suitable beam-free region downstream of a stripping foil and of the quality of the foil stripped beam. These were reported in Ref. 6 and since that time the driver has been installed semi-permanently in the cyclotron, Fig. 6. Experiments performed with both the driver and an electrostatic deflector culminated in the observation of an extractable H^- beam clearly separated from the circulating beam by over 10 mm 1.5 turns downstream from the septum protection foil, Fig. 9. The base width of the H^- beam was 7 mm; the extraction efficiency of the 1 mm foil-deflector combination was 85% for a 1 μA beam at a 1 kHz 5% duty cycle. That is for a low power 450 W beam with the ion source and space charge conditions of a 20 μA beam. The location of the measurement is close to that intended for the prototype magnetic septum channel.

The bevel gear drive mechanism which positions the forward end of the deflector stripped at the start of this experiment. The driver was tuned to present a density minimum at the frozen deflector rather than the latter moved to the optimal minimum. The measured 85% efficiency is exactly the value computed for a driver field of 60 (V/mm)m. The efficiency for the optimal conditions with a 1 mm wide foil is computed to be 90%. The beam was vertically misaligned at the location of the deflector and experienced only about 90% of the available deflecting field of 3.2 kV/mm. The bevel gear drive will be replaced by one using a non-magnetic chain; a section is presently being installed in the cyclotron to check operation. The entire deflected beam will be extracted during the next deflector

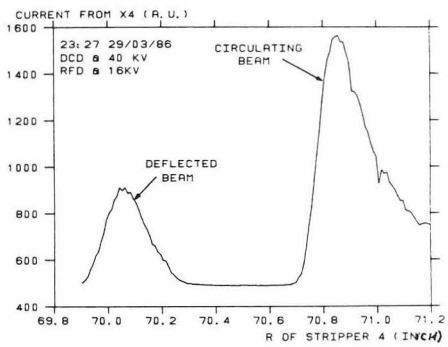

Fig. 9. Intensity distribution of deflected and circulating beams (2π+170°) downstream of the electrostatic deflector exit. Note a) zero offset (480 a.u.) on current amplifer, b) R-coordinate of stripper foil is (-1.1*geometric radius).

experiment to observe behavior at power levels higher than can be dissipated on the internal cyclotron probes.

At present about ±20° rf phase acceptance is required to deliver 100 μA H^- ions. This may decrease with the planned commissioning of a cusp H^- source and auxiliary cavities. Trim coils were used to generate a phase excursion, for a beam with width ±4°, at the resonance and beyond. The resulting density distributions are given in Fig. 10. The depth of the minima are fairly independent of phase; however the radial length of a precession cycle shortens as φ departs from isochronism. Thus, for a very wide phase band only the first minima are suitable for extraction. The stability is excellent since the significant turn number is measured from the resonance not from injection. The addition of one auxiliary cavity will approximately halve the number of turns in the resonance while doubling ΔR from acceleration, Fig. 2. The efficiency is similar but the precession period radial length is doubled and with phase width compression offers the possibility of extraction at higher energy.

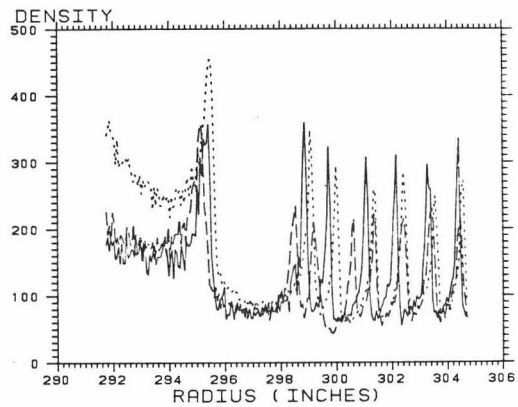

Fig. 10. Beam density vs radius for different phase histories in the resonance and precession region. The central phases extend over ~60°; about 40° is required to contain 100 μA.

Proton Accumulation

In the past beams of lower power have been injected into a ring, coasted until de-bunched, and then re-bunched as the ring rf voltage was brought on. The injector and ring rf systems are independent; however the capture efficiency is $\sim 2/\pi$, the remainder lying outside the separatrix and being lost to the beam pipe. Attempts to increase this with bucket heights much greater than the beam energy spread lead to distortion in $(E-\phi)$ space and an inhomogeneous line density. To eliminate this loss TRIUMF proposes to inject directly into buckets formed by 3 cavities each with 192 kV. No net acceleration would occur, the synchronous phase $\phi_s=0$. These create a longitudinal acceptance similar to that of the booster synchrotron and larger than the TRIUMF emittance. The power can accommodate voltages induced in the cavities by the accumulated beam. The anticipated tune shift for 1.25×10^{13} protons is $\lesssim 0.2$, note that this imposes a constraint on local density. The ring rf must be a multiple of the cyclotron frequency, 46 MHz was chosen and the two must be locked in phase. The ring circumference was chosen to have an odd number, 45, of buckets, each receives beam on alternate turns. A programmed deflection at the ion source, or elsewhere, leaves 5 adjacent buckets empty to provide a rise time for the kicker magnet which switches the beam into the booster synchrotron over one turn. The charge changing foil is positioned to one side of the beam pipe and a closed orbit bump with betatron and synchrotron oscillations is employed to

reduce the number of particle-foil interactions to ~200 from a potential maximum of 20,000. This is described more fully below.

The beam line between the cyclotron and accumulation ring can use site standard components. The maximum magnetic field should be < 0.5 T for a dissociation of < 10^{-5}/m length. The methods for improving extraction efficiency increase the dispersion of the extracted H^- beam several-fold. Some compensation may be obtained within magnetic channels, the rest should be at the cyclotron/beam line matching section for achromatic low loss transport. The section matching to the accumulator should focus the emittance onto a spot 3 mm diameter and provide some controlled mismatch in (x,x') and (E,ϕ) space to minimise foil interactions.[11] Since accelerating cavities may alter the central energy by 0.5% a section of laminated magnet may be necessary to conserve optics. A pulsed transverse strong deflector may be necessary to ensure five completely empty buckets for the ring extraction kicker rise time.

Beam-foil Interactions

A carbon foil has been assumed for the following study because of its availability, its emissivity and low atomic number. The thickness required to strip more than 99% of H^- to H^+ is in the region of 250 μg/cm^2. The first dipole field encountered will separate protons from any residual H^0 which then proceed, through diagnostic and interlock equipment, to a shielded dump. In a magnetic field free region the electrons may be swept off the foil and the power into the foil is chiefly from the circulating, stored, proton beam. The energy loss per passage follows a Landau distribution with a mean loss of 640 eV, most likely loss of 300 eV and a maximum loss of 1.2 MeV. The average number of angular scattering events is 4 per traversal. Plural scattering tables may be used or alternatively a single scattering applied four times. Interestingly there is no interaction with the atomic electrons for about 4% of the traversals. Nuclear scattering cross-sections are far below electron cross-sections, and since the scattering angle is larger they are assumed to lead to proton loss.

The temperature dependence of the rate of evaporation, or the vapour pressure, of carbon is well known. Assuming an emissivity of 0.8 a constant power input equivalent to 2,500 traversals/ proton or 0.35 A will evaporate 20 μg/cm^2 each hour over a beam spot 100 mm^2.

Primary and secondary collisions that impart > 30 eV can displace a carbon atom from its site in the lattice. At the end of their life the extraction foils used at 140 μA and 500 MeV and those used at 200 μA and 26 MeV in an isotope production cyclotron (CP-42) are buckled at the point of beam impaction. The exposure is 4×10^4 μA h in a spot 2×10 mm^2 at 500 MeV and 4×10^3 μA h at 26 MeV. This ratio of 10 is similar to that of the stopping power ratio (7.6). The dose corresponds to 3 or 4 displacements per atom and electron diffraction studies[12] of used foils show evidence of basal plane shrinkage typical of irradiation and graphitization of the 26 MeV foils. The latter occurs at temperatures above 2200° C, the 500 MeV and accumulator foils operate at lower temperature and irradiation effects imply < 250 traversals/proton for a lifetime of 10 h. The radiation lifetime varies inversely with dose until τ=1 h at which point thermal effects predominate.

Accumulation Procedure

The procedure should ensure that < 250 traversals occur per proton, that the local density never generates excessive space charge forces and that the final accumulated distribution matches the booster acceptance. A suitable procedure is described in Ref. 11. At the start of the accumulation process the incoming beam energy is adjusted to be 2.5 MeV above the ring synchronous energy. The beam will be injected into the upper part of the longitudinal acceptance and begin to execute a synchrotron oscillation. If the lattice has dispersion η at the injection point then the orbit is displaced laterally by $\Delta x=\eta(s)\Delta p/p$. If at the same time small laminated magnets are used to produce a closed orbit bump, or lateral displacement, Δx_{co} at the foil location then the central orbits for all energies are displaced from the beam pipe axis. Finally beam and foil are themselves displaced laterally a small distance Δx_β so that the injected beam performs a small betatron oscillation about the (E_s+2.5 MeV) orbit. The situation is illustrated in Fig. 11. The horizontal co-ordinate for the centre of the incoming beam is $x=\Delta x_{co} + \eta\Delta p/p + \Delta x_\beta$, this stays the same throughout accumulation. Both synchrotron and betatron oscillation serve to periodically move the beam off the foil.

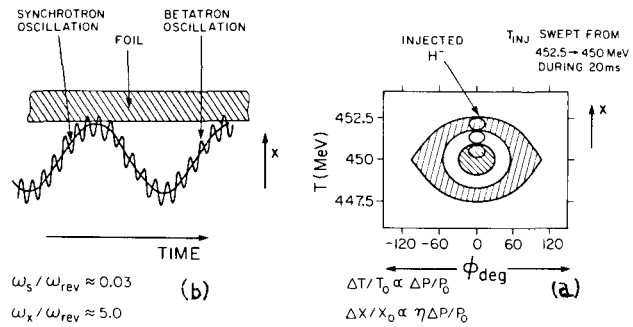

Fig. 11. a) Illustrates accumulation in longitudinal space as the energy of the injected beam decreases. b) A stroboscopic picture at the foil azimuth showing the position of a particle undergoing synchrotron and betatron oscillations and the consequent reduction in foil impacts.

As accumulation proceeds the incoming energy is lowered towards the synchronous value and the closed orbit displacement falls toward the ring axis; the displacement of the beam injected initially falls below the foil radius when the change in Δx_{co} approximately equals the incoming beam width. The former may be achieved using cavities similar to those in the ring in the beam transfer line between the cyclotron and ring; the latter by reducing the field in the bump magnets. At the end of injection the longitudinal amplitude is small and the horizontal betatron amplitude large. The flux of beam through the foil is kept constant during accumulation; however the first several thousand turns are made with a hollow longitudinal phase space, i.e. with density peaking at the front and rear of the bunch. The ideal, stable, parabolic distribution has space charge forces directed away from the centre of the bunch. A hollow distribution has forces directed away from and to the centre. In addition fast beam pickup detectors, which may be used for feedback purposes, sense two peaks per bunch. These may not be serious concerns. The 50 Hz ISIS spallation source in the U.K. captures a de-bunched beam and has a line density with several, separate, strong peaks. The intensity was increased from 10 to 30 μA with a simple feed-forward system[13] that incorporated a 1 MHz filter in the detection circuit and essentially identified the phase of the main Fourier component. Since the beam density is low when the longitudinal distribution is hollow the beam loading effect should be small. The

beam is also swept vertically, not to reduce foil interactions, but to reduce power density and to fill the vertical acceptance.

Should the phase between ring rf and incoming beam be swept instead of the energy the foil must extend from $(x_{co}+x_{\beta})$ outward and experience more traversals or a thin ribbon foil, unsupported on either side, must be used. Injection at energies above or below the synchronous energy have a slightly different behaviour. The energy lost in foil traversals increases the central population for the former and enlarges E-ϕ space for the latter. Pollock[14] points out that this will be accompanied by a similar effect with opposite sense in (x,x') space; however the relative magnitude of the latter is small for the large beam of the A-ring.

Computer Simulation

A Monte Carlo program ACCSIM has been written to yield density distributions for analytically intractable cases. The program tracks particles by matrix multiplication. Although the complete lattice is read in the accumulation is usually calculated by advancing the particles one complete turn, testing for a foil interaction and altering (x',y',E) if one occurs. The energy lost in the foil is binned for eventual thermal calculations. New particles, within the incoming emittance, are introduced into the computation every ten or so turns. Care is taken to avoid stroboscopic effects. The intermediate accumulated arrays are written out periodically and these are tracked element by element for at least one synchrotron oscillation to check for excessive beam amplitudes or loss. The accelerating voltage is sufficiently high that the kick and associated x shift must be applied at locations 120° apart to avoid skewing the accumulated (E-ϕ) distribution. Space charge effects are not included at the moment.

The final distributions in phase space and real space are given in Fig. 12. The average proton interacts about 300 times and the power input is estimated to be about 15 W over an area 5×10 mm. This is lower than the power density in TRIUMF. The closed orbit and energy (452.5 to 450.5) were ramped linearly, although non- linear ramping is expected to be beneficial. Oscillatory ramping, a few cycles each 20 ms period, may also be beneficial in reducing local density peaks and in accommodating beam fluctuations. Injection from a linear accelerator should last several hundred microseconds to obtain a similar performance.

Conclusion

The task of extracting a 100 μA H^- beam from the TRIUMF cyclotron is solved in principle and, although development work is necessary, no intractable problems are envisaged for the hardware. The new technique of generating a coherent radial amplitude by means of an rf field provided a cheap (80 kC$) and fast (6 month) approach to extraction efficiency. Over the longer term the tripling of the energy gain will provide an operationally more convenient approach. The accumulation of this beam over 20,000 turns is possible to first order, and from synchrotron experience it is felt that the process will be stable to space charge forces and to the inevitable fluctuations in the incoming H^- beam current. However the simulation processes have not yet included these effects nor the imperfections that might arise from non-linear fields introduced by the closed orbit bump process. The instabilities of the basic ring are thought to be mild.

The present experimental pattern consists of short runs at the end of long maintenance periods, followed by the removal of apparatus interfering with production operation. A continuation of this will permit development of H^- extraction equipment, tests at currents up to 10 μA, and the installation and commissioning of auxiliary accelerating cavities.

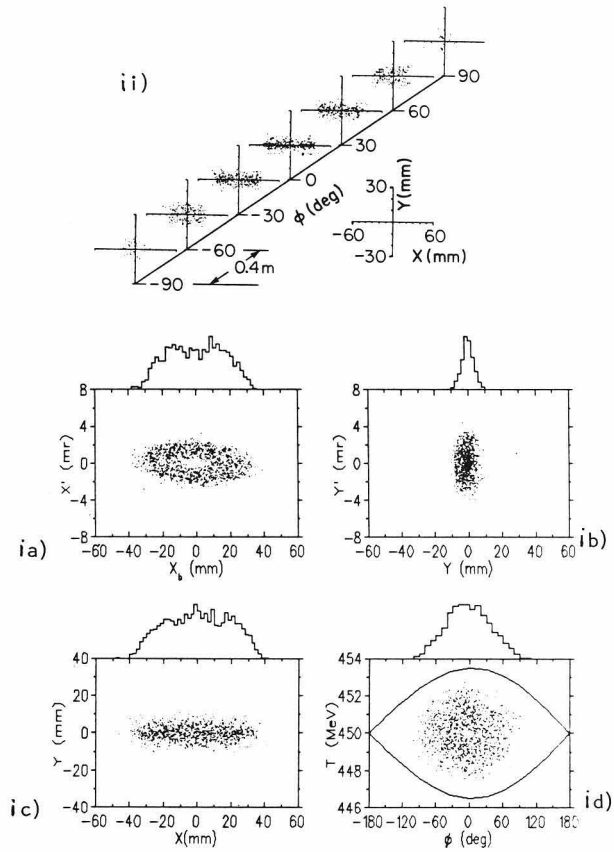

Fig. 12. Scatter plots of beam accumulated after 20,000 turns. i) a,b,d horizontal, vertical and longitudinal phase space. 1) c and ii) real space.

Acknowledgements

The author would like to thank Messrs. F. Jones, R. Lee, R. Laxdal and M. Sivaramakrishnan for help in figure preparation and for the generous co-operation of colleagues whose work is included here. Their names may be found in the references.

References

1. KAON Factory Proposal, TRIUMF, September 1985.
2. R. Laxdal et al., IEEE NS-30, 2013, 1983.
3. W. Joho, IEEE NS-30, 2083, 1983.
4. L.P. Robertson et al., V Int. Cycl. Butterworth, p.245, 1971.
5. W. Joho, V Int. Cycl. Conf., Butterworth 1971, p.159.
6. R.E. Laxdal and G.H. Mackenzie, IEEE NS-32, 2453, 1985.
7. R.E. Laxdal et al., this conference.
8. R. Worsham, private communication, 1985.
9. R. Trelle and M. Zach, private communication, 1985.
10. E. de Vita, Proceedings of 9th Int. Conf. on Magnet Technology and TRI-DN-84-27.
11. D. Raparia, C.W. Planner, G.H. Mackenzie and J.R. Richardson, IEEE, NS-32, 2456, 1985.
12. W. Cranton - TRIUMF/Surrey industrial experience report.
13. I. Gardner, private communication, 1986.
14. R.E. Pollock, private communication, 1986.